Thermoelastic Dynamic Analysis of Microbeams Under Laser Pulse

Mengyao Cui[1,2], Ming He[1,2], Yanbing Liang[2,*]
[1]*Hebei Key Laboratory of Data Science and Application, North China University of Science and Technology, Tangshan, Hebei, China*
[2]*College of Science, North China University of Science and Technology, Tangshan, Hebei, China*
**Corresponding Author*

Abstract: In this paper the thermoelastic dynamic response of microbeam under laser pulse and the influence by noise interference are investigated for the first time. the governing equations of the microbeam are established by the fractional order two-phase hysteresis model and the Kelvin-Voigt model, and are solved using the shifted Chebyshev polynomials algorithm. Finally, some numerical simulations are provided, which demonstrate the validity the efficiency and robustness by the proposed method.

Keywords: Microbeams; Fractional Order; Shifted Chebyshev Polynomials; Thermoelasticity

1. Introduction

Microbeams are significant on the micro-nanoscale, and are employed extensively in a number of fields, including sensing, actuation and precision control [1]. Although the mechanical properties of viscoelastic materials have been well studied, research on their thermoelastic behaviour remains relatively understudied. Along with the accelerated advancement of laser technology, there has been a growing focus on the utilisation of laser load in viscoelastic structures. Putting a specific degree of laser loading on the microbeam causes increasing the temperature of the microbeam structure, resulting in thermal expansion and subsequent changes in strain and deformation of the microbeam [2].

Fourier's law of heat conduction is a foundational law that describes the heat conduction behaviour in solids. However, it has been observed that the law may have limitations in describing the heat conduction behaviour of complex materials. To address this, two-phase hysteresis model [3] and fractional order have been introduced to better describe the dynamic behaviour of these materials [4-5].

$$\left(1+\tau_q D_t^{\alpha}\right) q=-K\left(1+\tau_T D_t^{\alpha}\right) \nabla T \quad (1)$$

where K is the thermal conductivity of the material.

The fractional order two-phase hysteresis model is a more comprehensive analytical tool for examining the temperature change and heat transfer behaviour of materials subjected to thermal shock. In this paper, Caputo fractional-order derivatives [6-7] are employed to more accurately capture the dynamic response properties of the materials. the shifted Chebyshev polynomial algorithm is used to solve governing equations of the viscoelastic microbeam in the time domain directly and discretises it into a set of linear algebraic equations. Subsequently, numerical simulations of the microbeams are carried out using the MATLAB programme.

2. Modeling

The equations of motion and fractional order heat transfer equations are derived as follows by establishing the thermal stresses defined by the Kelvin-Voigt model [8], bending moment equations, the law of conservation of energy and the fractional order two-phase hysteresis model.

$$\left(1+\tau_d \frac{\partial}{\partial t}\right)\left[\frac{\partial^4 \omega}{\partial x^4}+\frac{24\alpha_T}{h\pi^2}\frac{\partial^2 T}{\partial x^2}\right]+\frac{\rho A}{EI}\frac{\partial^2 \omega}{\partial t^2}+\frac{\sigma_0 A}{EI}\frac{\partial^2 \omega}{\partial x^2}=0, \quad (2)$$

$$\begin{gathered}\left(1+\tau_T D_t^{\alpha}\right)\left(\frac{\partial^2}{\partial x^2}-\frac{\pi^2}{h^2}\right)T+\frac{\pi^2}{2Kh^2}\left(1+\tau_q D_t^{\alpha}\right)\int_{-2/h}^{2/h} zF dz= \\ \left(1+\tau_q D_t^{\alpha}\right)\left[\frac{\rho C}{K}\frac{\partial T}{\partial t}-\frac{\alpha_T \pi^2 h T_0 E}{24K}\left(1+\tau_d \frac{\partial}{\partial t}\right)\left(\frac{\partial^3 \omega}{\partial t \partial x^2}\right)\right]\end{gathered}. \quad (3)$$

It is assumed that the microbeam is subjected to a load from a heat source applied in the form of laser pulse [9-10]: $F=F_0\delta(x-vt)F(t)$, where F_0 represent the power density.

3. Solution Process

3.1 Shift Chebyshev Polynomials

The shifted Chebyshev polynomials is derived the recurrence relation in the interval $[0, L]$ [11]:

$$D_{i+1}(t) = 2\left(\frac{2t}{L} - 1\right) D_i(t) - D_{i-1}(t), \quad i \in N_+ . \quad (4)$$

The vector consisting of the shifted Chebyshev polynomials is given by

$$\Phi_n(t) = \left[D_0(t), D_1(t), \ldots, D_n(t)\right]^T = KG_n(t) ,$$

where $G_n(t) = [1, t, t^2, \cdots, t^n]^T$, $K = \left[k_{ij}\right]_{i,j=0}^{n}$, where $k_{ij} = 1$ if $i = j = 0$; where $k_{ij} = 0$ if $i < j or i < 0 or j < 0$; $k_{ij} = 2\left(\frac{2}{L} k_{i-1,j-1} - k_{i-1,j}\right) - k_{i-2,j}$ else.

3.2 Function Approximation

The truncated sequence of two-dimensional continuous function $\omega(x,t)$ can be expressed:

$$\omega(x,t) \approx \sum_{i=0}^{n} \sum_{j=0}^{n} u_{ij} D_i(x) D_j(t) = \Phi_n^T(x) U \Phi_n(t) , \quad (5)$$

where $U = \left[u_{ij}\right]_{i,j=0}^{n,n}$,

$$u_{ij} = \frac{1}{k_i k_j} \int_0^L \int_0^T \omega(x,t) D_i(x) D_j(t) \omega_L(x) \omega_T(t) dt dx .$$

Similarly,

$$T(x,t) \approx \sum_{i=0}^{n} \sum_{j=0}^{n} w_{ij} D_i(x) D_j(t) = \Phi_n^T(x) W \Phi_n(t) .$$

3.3 Differential Operator Matrices of Shifted Chebyshev Polynomials

Definition 1 The first order differential operator matrix H_x^1 of the shifted Chebyshev polynomials $\Phi_n(x)$ is defined as follows:

$$\Phi'_n(x) = (KG_x(x))' = K(G_x(x))' = K(K_x^{-1}\Phi_n(x))' = KPK^{-1}\Phi_n(x) = H_x^1\Phi_n(x), \quad (6)$$

where $P = \left[p_{ij}\right]_{i,j=0}^{n}$, where $p_{ij} = i$ if $i = j+1$; $p_{ij} = 0$ else.

The integer differential operators matrix of the shifted Chebyshev polynomials is defined by: $\Phi_n^{(m)}(x) = \left(KPK^{-1}\right)^m \Phi_n(x) = H_x^m \Phi_n(x)$.

Definition 2 The variable fractional order differential operator's matrix $H_t^\alpha(t)$ of the shifted Chebyshev polynomials $\Phi_n(x)$ is defined as follows:

$$D_t^\alpha \Phi_n(t) = KD_t^\alpha(G_t(t)) = KP^\alpha G_t(t) = KP^\alpha K^{-1}\Phi_n(t) = H_t^\alpha \Phi_n(t), \quad (7)$$

where $p^\alpha = \left[p_{ij}^\alpha\right]_{i,j=0}^{n}$, where $p_{ij}^\alpha = 0$ if $i \neq j$ or $i = j = 0$; where $p_{ij}^\alpha = \frac{\Gamma(i+1)}{\Gamma(i+1-\alpha)}$ else.

3.4 Equation Discretisation

Based on the above differential operator matrixs, the microbeam control equations (2) and (3) can be transformed into the following operator matrix forms:

$$\Phi_n^T(x)\left(H_x^4\right)^T U\Phi_n(t) + \tau_d \Phi_n^T(x) H_x^4 \left(H_x^4\right)^T U H_t^1 \Phi_n(t) + \frac{24\alpha_T}{h\pi^2}\Phi_n^T(x)(H_x^2)^T W\Phi_n(t) + \frac{24\alpha_T}{h\pi^2}\tau_d \Phi_n^T(x)(H_x^2)^T W H_t^1 \Phi_n(t) + \frac{\rho A}{EI}\Phi_n^T(x) U H_t^2 \Phi_n(t) + \frac{\sigma_0 A}{EI}\Phi_n^T(x)(H_x^2)^T U\Phi_n(t) = 0, \quad (8)$$

$$\Phi_n^T(x)(H_x^2)^T W\Phi_n(t) + \tau_T \Phi_n^T(x)(H_x^2)^T W H_t^\alpha \Phi_n(t) - \frac{\pi^2}{h^2}\Phi_n^T(x) W\Phi_n(t) - \tau_T \frac{\pi^2}{h^2}\Phi_n^T(x) W H_t^\alpha \Phi_n(t) - \frac{\rho C}{K}\Phi_n^T(x) W H_t^1 \Phi_n(t) + \frac{\alpha_T \pi^2 h T_0 E}{24K}(\Phi_n^T(x)(H_x^2)^T U H_t^1 \Phi_n(t) + \tau_d \Phi_n^T(x)(H_x^2)^T U H_t^2 \Phi_n(t)) + \frac{\alpha_T \pi^2 h T_0 E}{24K}\tau_q(\Phi_n^T(x)(H_x^2)^T U H_t^\alpha H_t^1 \Phi_n(t) + \tau_d \Phi_n^T(x)(H_x^2)^T U H_t^\alpha H_t^2 \Phi_n(t)) - \tau_q \frac{\rho C}{K}\Phi_n^T(x) W H_t^\alpha H_t^1 \Phi_n(t) - \frac{\pi^2}{2Kh^2}(1 + \tau_q D_t^\alpha)\int_{-2/h}^{2/h} zF dz = 0. \quad (9)$$

According to the method of matching points, the variable (x,t) is discretised into the variable (x_i, t_j) , $x_i = \frac{2i-1}{2m}L, i = 0,1,2,\cdots,m-1$, $t_j = \frac{2j-1}{2m}T, j = 0,1,2,\cdots,m-1$. The numerical solution of the control equations (2) and (3) is then obtained through the MATLAB programme.

4. Numerical Results

The Lord-Shulman fractional order thermoelastic model (abbreviated as FVLS, $\tau_\theta = 0$) and the fractional order thermoelastic two-phase lag model (abbreviated as FVDPL, $\tau_\theta > 0$) are considered [13]: the parameters of the microbeam are $E = 1800Gpa$,

$\rho = 1930kgm^{-3}$, $\alpha_t = 2.59K^{-1}$, $K = 317Wm^{-1}K^{-1}$, $C = 130Jkg^{-1}K^{-1}$, $\nu = 0.44$, $T_0 = 293K$ [12].

4.1 Comparison of Microbeams Deflection Response Based Two Models

Figure 1 demonstrates the trends of the FVLS and FVDPL models are similar, the peak value of the deflection is significantly higher in the FVDPL model [13]. Specifically, Figure 1(a) shows the deflection variation of the FVLS model with noise interference and no interference conditions, with almost the same results; Figure 1(b) further validates this conclusion and proves the stability of the proposed algorithm.

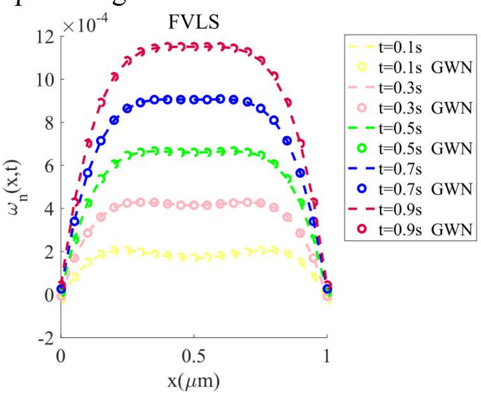

(a) Deflection variation with FVLS model.

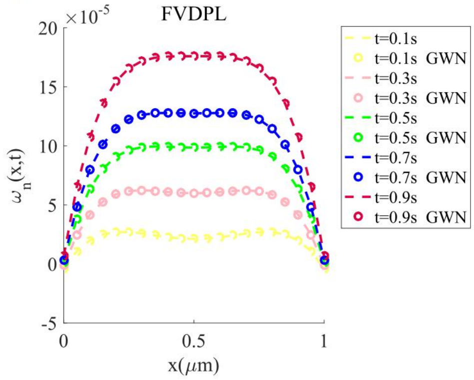

(b) Deflection variation with FVDPL model.

Figure 1. Comparison of Microbeam Deflection Under Two Models

4.2 Comparison of Microbeams Temperature Response Based Two Models

Figure 2 illustrates the temperature variation trend is similar for both models, but the peak temperature value is significantly higher under the FVLS model. Figure 2(a) illustrates that the temperature variation of the FVLS model is essentially identical under both noise-disturbed and non-disturbed conditions [14]. This outcome serves to reinforce the veracity of the algorithm proposed in this paper.

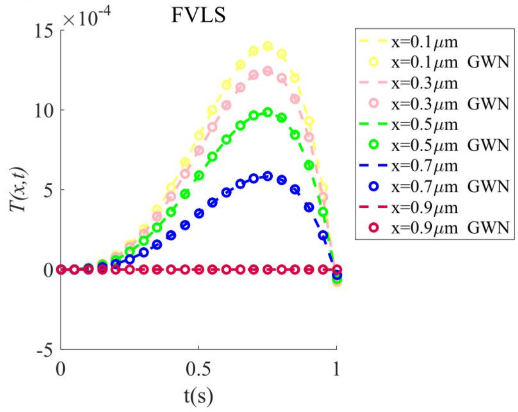

(a) Temperature variation with FVLS model

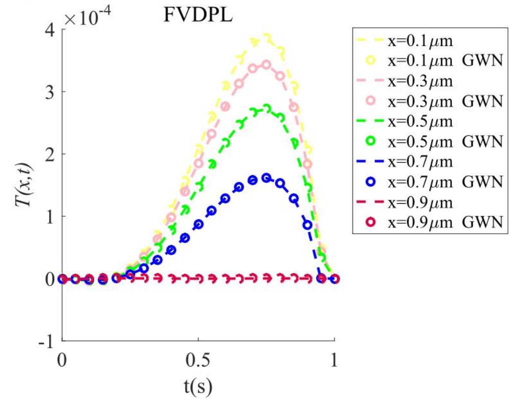

(b) Temperature variation with FVDPL model

Figure 2. Comparison of Microbeam Temperatures Under the Two Models.

5. Conclusion

(1) The peak of the microbeam deflection under the FVDPL model is markedly higher than that under the FVLS model, whereas the peak of the temperature under the FVLS model is significantly higher than that under the FVDPL model.

(2) The algorithm proposed in this paper has stability and reliability that can effectively resist noise interference.

Reference

[1] Dang R, Cui Y, Qu J, Yang A, Chen Y. Variable fractional modeling and vibration analysis of variable-thickness viscoelastic circular plate [J]. Applied Mathematical Modelling, 2022, 110:767-778.

[2] Tang D W, Araki N. Non-fourier heat condution behavior in finite mediums under pulse surface heating [J]. Materials Science and Engineering, A, 2000, 292(2):173-178.

[3] Ezzat M A, Othman M I, El-Karamany A M S. State space approach to two-dimensional generalized thermo-viscoelasticity with two relaxation times [J]. International journal of engineering science, 2002, 40(11):1251-1274.
[4] Yang W, Chen Z. Investigation of transient thermal-mechanical behavior of a cracked viscoelastic material using time-fractional dual-phase-lag theory [J]. Theoretical and Applied Fracture Mechanics, 2020, 106:102500.
[5] Othman M I A, Song Y. Effect of rotation on plane waves of generalized electro-magneto-thermoviscoelasticity with two relaxation times [J]. Applied Mathematical Modelling, 2008, 32(5):811-825.
[6] Betancur-Herrera D E, Muñoz-Galeano N. A numerical method for solving Caputo's and Riemann-Liouville's fractional differential equations which includes multi-order fractional derivatives and variable coefficients. Communications in Nonlinear Science and Numerical Simulation, 2020, 84:105180.
[7] Podlubny I. Fractional differential equations: an introduction to fractional derivatives, fractional differential equations, to methods of their solution and some of their applications. Elsevier, 1998.
[8] Biot M A. Theory of stress - strain relations in anisotropic viscoelasticity and relaxation phenomena. Journal of applied physics, 1954, 25(11):1385-91.
[9] Ma J, Sun Y, Yang J. Analytical solution of dual-phase-lag heat conduction in a finite medium subjected to a moving heat source. International Journal of Thermal Sciences, 2018, 125:34-43.
[10] Xia R, Tian X, Shen Y. Dynamic response of two-dimensional generalized thermoelastic coupling problem subjected to a moving heat source. Acta Mechanica Solida Sinica, 2014, 27(3):300-5
[11] Wang Lei, Chen Yiming, FENG Junyao. Numerical Analysis of fractional-order viscoelastic Euler-Bernoulli Beams [J]. Journal of Liaoning Technical University (Natural Science Edition), 2020, 39(05):471-476.
[12] Alizadeh Hamidi B, Hosseini SA. An exact solution on gold microbeam with thermoelastic damping via generalized GreenNaghdi and modified couple stress theories. Journal of Thermal Stresses, 2020, 43(2):157-74.
[13] Abouelregal AE, Alesemi M. Vibrational analysis of viscous thin beams stressed by laser mechanical load using a heat transfer model with a fractional Atangana-Baleanu operator. Case Studies in Thermal Engineering, 2022, 34:102028.
[14] Qu J, Zhang Q, Yang A, Chen Y, Zhang Q. Variational fractional-order modeling of viscoelastic axially moving plates and vibration simulation. Communications in Nonlinear Science and Numerical Simulation, 2024, 130:107707.